



Cite this: *Phys. Chem. Chem. Phys.*,  
2015, 17, 21709

## Electrochemical 'bubble swarm' enhancement of ultrasonic surface cleaning†

P. R. Birkin,<sup>\*a</sup> D. G. Offin,<sup>a</sup> C. J. B. Vian<sup>a</sup> and T. G. Leighton<sup>b</sup>

An investigation of surface cleaning using a swarm of gas bubbles within an acoustically activated stream is presented. Electrolysis of water at Pt microwires (100  $\mu\text{m}$  diameter) to produce both hydrogen and oxygen bubbles is shown to enhance the extent of ultrasonic surface cleaning in a free flowing water stream containing an electrolyte (0.1 M  $\text{Na}_2\text{SO}_4$ ) and low surfactant concentration (2 mM SDS). The surfactant was employed to allow control of the average size of the bubble population within the swarm. The electrochemical bubble swarm (EBS) is shown to perturb acoustic transmission through the stream. To optimise the cleaning process both the ultrasonic field and the electrochemical current are pulsed and synchronized but with different duty cycles. Cleaning action is demonstrated on structured surfaces (porcine skin and finger mimics) loaded with fluorescent particles. This action is shown to be significantly enhanced compared to that found with an inherent bubble population produced by the flow and acoustic regime alone under the same conditions.

Received 21st May 2015,  
Accepted 16th July 2015

DOI: 10.1039/c5cp02933c

www.rsc.org/pccp

### Introduction

Cleaning at a solid/liquid interface plays a vital role in many human activities. Whether this is in the production of food, fabrication of electronic components, sterilisation in the health-care sector or as a basic hygiene requirement, the same issue occurs: how to clean the material involved in an efficient manner but without degrading or damaging it? As such, many technological approaches have been developed. While many of these are undoubtedly successful, improvements in energy efficiency, reductions in water usage, better cleaning efficacy and reductions in chemical additives used are desirable attributes of new technologies within this sector compared to the standard practice. Amongst the many techniques employed to clean surfaces, ultrasound<sup>1–8</sup> has many appealing qualities. This technology uses the action of bubbles driven by ultrasonic irradiation of the media to clean an interface. Ultimately it is the interaction of sound and bubbles<sup>9</sup> that drives the cleaning action although the exact mechanism may vary depending on the conditions employed.

Cavitation is certainly a key factor, as the unusual physical<sup>10,11</sup> (for example shock waves, shear<sup>12,13</sup> and erosion<sup>14–17</sup>) as well as the chemical effects<sup>18–23</sup> (the production of strong oxidants for example) are useful in this role. Ultrasonic cleaning has the

advantage that it is relatively simple to deploy with the ubiquitous ultrasonic cleaning bath common in many academic, medical, industrial and even domestic environments. However, this technology also has limitations. These will include: the presence of 'hot' and 'cold' spots of cavitation activity (meaning that without mitigation some regions might not be cleaned); perturbation and quenching, by immersion of the object to be cleaned, of the sound field that was measured (*e.g.* for calibration purposes) prior to its immersion<sup>10</sup> such that the calibration is misleading; the use of chemical additives to enhance the action in some systems, increasing cost and complicating subsequent water treatment; the size restrictions imposed by the bath itself (limiting the size of object that can be cleaned); the inability of the bath to reach into complex geometries (such as pipework); and the possible re-deposition of contaminant from one location to another in the essentially stagnant media. Clearly, the need for immersion may be viewed as limiting, hence alternative strategies should be considered. One such alternative strategy is the employment of an acoustically activated low velocity stream of fluid impinging on the interface to be cleaned.<sup>24,25</sup> Key to this concept is the generation of suitable ultrasonic cleaning conditions at the solid/liquid interface presented to the device. This is non-trivial as it requires the efficient transmission of acoustic energy down a flowing stream of fluid (or waveguide) from a suitable source.<sup>26,27</sup> However, this has been achieved through the careful choice of device design, materials, acoustic frequency, an understanding of bubble population effects and control of the fluid stream. Details of this development<sup>24,25</sup> and the devices' performance in pure water can be found elsewhere<sup>28</sup> and an image of a device is shown in Fig. 1. In effect an ultrasonic

<sup>a</sup> Chemistry, Natural and Environmental Sciences, University of Southampton, Southampton, SO17 1BJ, UK. E-mail: prb2@soton.ac.uk

<sup>b</sup> Institute of Sound and Vibration Research, Engineering and the Environment, University of Southampton, Southampton, SO17 1BJ, UK

† Electronic supplementary information (ESI) available: Movies from Fig. 3(c) and (d) are provided. See DOI: 10.1039/c5cp02933c

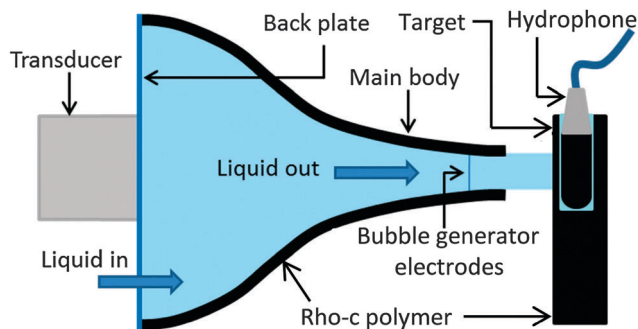


Fig. 1 Schematic cross-section of the device architecture. In this case the target is shown as an embedded hydrophone. Note that in this case the device is shown with the transducer nozzle axis arranged horizontally. However, it can be mounted in other orientations, for example the transducer/nozzle axis can be arranged vertically as shown in Fig. 3.

cleaning system at the end of a fluid stream has been produced without some of the limitations associated with cleaning bath technology<sup>25</sup> and without the aerosol, spray, high water usage or power consumption of a high pressure jet. Nevertheless, this technology could be improved. For example, the cleaning action relies on the interaction between the sound field and the bubble population at the solid/liquid interface. Clearly in pure water this is reliant on the inherent bubble population generated by the device. In many situations this will be sufficient. However, one could imagine other applications where the introduction of activated bubble swarms or clouds could be advantageous. For example, if the bubble content of the liquid is low, cleaning may be inhibited by the absence of a myriad of bubbles even though the acoustic conditions are suitable. In addition, for fragile interfaces (for example skin or electronic components), the acoustic field should be minimised to avoid unnecessary damage. Under either of these conditions the introduction of activated bubble swarms where high shear<sup>12,13,29</sup> is produced through violent bubble motion could be beneficial. This paper investigates whether there is advantage to be had by adding a controlled bubble population to the stream by performing electrolysis at electrodes shown at the tip of the device in Fig. 1. This paper will report on the effectiveness of adding an electrochemical bubble swarm (EBS) on surface cleaning, the effect of this cloud on ultrasonic transmission within the stream and the limitations of this approach will all be demonstrated and discussed.

## Experimental

The experimental setup consisted of a flow system, horn (or cone) structure, nozzle, power amplifier and control electronics. A cross-sectional schematic of the device is shown in Fig. 1. The device consisted of a main body, back plate and transducer (135 kHz). The main body of the structure was made from a cast moulded rho-c polymer (matched to the acoustic properties of water), which was attached to a circular polycarbonate back plate (thickness 1 mm) by means of epoxy resin (Araldite, Rapid). The body was axially symmetric and the wall had a sigmoidal cross section. The rho-c body was cast in a mould made from PTFE constructed by the University of Southampton

Mechanical Workshop. Note the ultrasonically activated stream (UAS) device is now available from Ultrawave Ltd (F0030001, StarStream). The UAS concept (with electrochemical bubble generation was reported in 2010/11).<sup>24</sup> Two bubble generation electrodes were made from platinum wire (100  $\mu\text{m}$  diameter, Advent Research Materials) each of which were  $\sim 10$  mm in length. These were positioned in the nozzle exit such that they were vertical and parallel to each other, separated by approximately 2 mm and 10 mm from the nozzle exit. An ultrasonic transducer was attached to the centre of the back plate using epoxy resin. The back plate had two inlets for liquid (each diameter 8 mm) and a bleed outlet (diameter 2 mm). The inlets and outlet were positioned on opposite sides of the transducer. The nozzle was mounted such that the inlets were at the bottom and the bleed outlet was at the top of the device. During operation the liquid from a tank was gravity fed to a centrifugal pump (Totton NDP 14/2) and then pumped through a flow meter (GEMS FT-110 Series) and into the nozzle.

After flowing through the nozzle and onto the target the liquid returned to the tank. The total volume of liquid was approximately 5 dm<sup>3</sup> and it was not temperature controlled. It is essential that the nozzle structure is full of liquid while it is in operation, and so the nozzle was orientated so that the bleed outlet was upper-most, allowing air to be expelled through this outlet. This is particularly relevant during the initialisation of the device, where the nozzle exit must be blocked after the flow has started, to allow air to exit the nozzle through the bleed outlet. When the nozzle exit was released it was found that the nozzle generally remained full of liquid and a small flow exited through the bleed and was returned to the tank by a tube.

The sinusoidal signal to the transducer was generated using a function generator (TTi TGA12101) and power amplifier (Brüel & Kjær Type 2713). The signal from the function generator was gated with a custom built set of control electronics, which also controlled the bubble generation. Bubbles were generated using a 24 V supply applied to the electrodes.

Acoustic pressures were measured using a Brüel & Kjær Type 8103 hydrophone and a charge amplifier (Brüel & Kjær Type 2635). The hydrophone used is relatively large compared with the stream diameter (hydrophone external diameter is 9.5 mm) and so a target was constructed using the same polymer that was used in the construction of the nozzle. This was a block measuring 100 mm  $\times$  64 mm  $\times$  25 mm. There was a cylindrical hole (10 mm diameter and 40 mm deep) in one of the long faces (100 mm  $\times$  25 mm face), positioned such that the centre of the hole was 7 mm from the front face (100  $\times$  64 mm face). The hydrophone was placed in the hole and surrounded with water. The block was placed in front of the nozzle so that the hydrophone was vertical and the stream impinged on the front face of the block in front of the acoustic centre of the hydrophone (see Fig. 1).

High-speed images of the output flow were recorded using a Photron Fastcam APX RS camera.

Hand mimics were made by creating a mould of a hand using Creaform casting paste and filling with rho-c polymer. Porcine skin samples were obtained from a supermarket product. The fluorescent tracer was Wash & Glow UV Germ Fluid

(Glowtec, a particulate based material). A couple of drops were applied to each sample, spread by hand and allowed to dry before use. Images of the samples were taken using a JAI CV-S3200 camera fitted with a Navitar 12 $\times$  zoom lens. Images were taken in the dark and illuminated with a UV lamp.

Re-passivation events detected by an aluminium surface were counted as a function of position of the electrode in the stream. The electrode was positioned roughly in the centre of the stream, 10 mm from the nozzle exit. The nozzle was then moved 6 mm down and 6 mm to the left, such that the electrode was out of the stream. Data were then collected at 169 positions (13  $\times$  13 matrix) with 1 mm resolution.

Separate experiments designed to investigate the effect of surfactant loading on the size of bubbles produced from 100  $\mu\text{m}$  diameter microwire electrodes was undertaken using a 1  $\text{cm}^2$  flow cell feeding into a thin layer section ( $\sim 1$  mm depth) through which the bubble clouds were imaged using the Photron Fastcam APX RS camera with the cell backlit to give a silhouette of the bubbles produced.

## Results and discussion

Fig. 2 shows the effect of EBS generation on the transmission of sound through the water column to a hydrophone placed within a rho-c polymer block (see Fig. 1 for configuration). Initially (before point A) the pressure detected by the hydrophone in the polymer block was of the order of 220 kPa (zero-to-peak) using the calibration data available. However, as soon as electrolysis

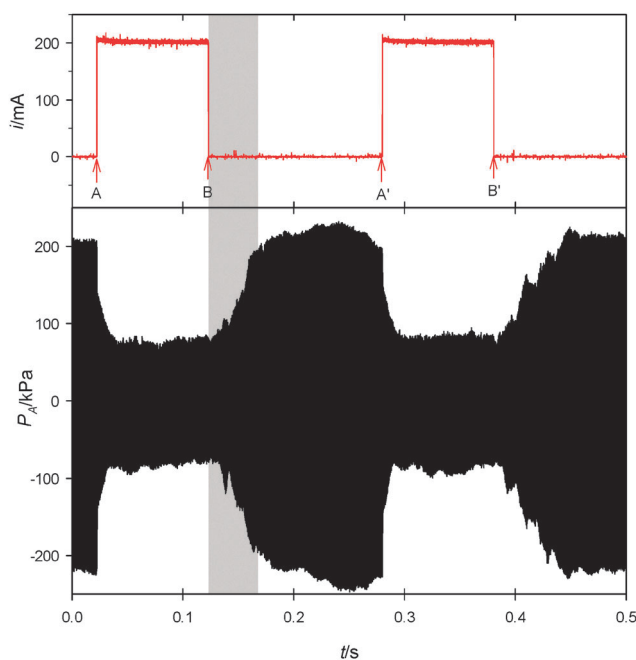
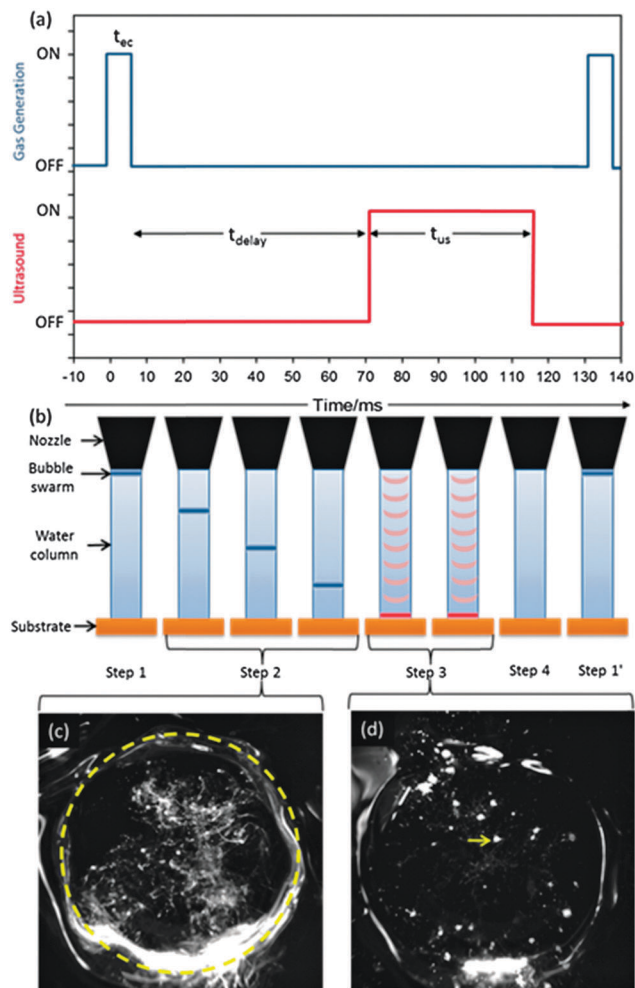


Fig. 2 Plot showing the effect of electrochemical bubble swarm generation on the acoustic transmission through the cone and fluid column to a hydrophone placed within a rho-c block (see Fig. 1(a)). Here the transducer was driven to produce a  $\sim 220$  kPa zero-to-peak acoustic field at the hydrophone (—). The electrochemical bubble swarm is then initiated at A and A' and terminated at B and B' (—).

is initiated at point A, strong perturbation of the pressure reaching the hydrophone was observed (note the Pt electrodes were placed 10 mm from the end of the nozzle). This perturbation occurs over  $\sim 10$  ms after which the pressure amplitude reaches  $\sim 70$  kPa (zero-to-peak) and remains at this level until the electrolysis of the fluid is terminated at point B. However, the acoustic pressure amplitude does not recover to its original value until 40–60 ms after the electrolysis of the system has been terminated (recovery is highlighted by the grey box, which covers 40 ms). This represents the time required to clear the bubbles from the fluid column between the generation electrodes and the surface of the rho-c block. This is reasonable given the linear flow rate ( $40 \text{ cm s}^{-1}$ ) and distance between the electrodes and the surface of the polymer block (20 mm). After these gas bubbles have cleared the pressure recovered to that seen before the bubble generation.

This process can then be repeated as subsequent pulses of bubbles are introduced through further electrolysis periods (see A' and B'). Clearly the introduction of gas bubbles in this manner reduced the pressure amplitude recorded at the hydrophone. This 'bubble gating' effect could be seen as detrimental to surface cleaning as both high acoustic pressure amplitudes and bubbles at the solid/liquid interface are needed for effective cleaning to be initiated. However, continuous electrochemical bubble generation results in the acoustic pressure amplitude reducing significantly. It is also likely that continuous acoustic excitation of the bubble swarm will change the bubble size distribution through coalescence, for example. Hence, an alternative strategy should be sought. In this case an approach has been adopted where electrochemical bubble generation is performed in a pulsed manner in coordination with the activation of the sound field. The EBS is generated and allowed to travel through the liquid to the surface to be cleaned in the absence of ultrasound. On arrival at the surface ultrasonic irradiation of the system is initiated. The EBS is then activated by sonic excitation of the system and cleaning can be triggered. Fig. 3 shows just such an approach including the timing of the bubble swarm and activation signal from the acoustic transducer employed (Fig. 3(a)), a schematic of the process (Fig. 3(b)) as well as images recorded with a high-speed camera (Fig. 3(c) and (d)). These images were taken 'up the stream' by directing a horizontal stream at a transparent interface. Fig. 3(c) shows a bubble cloud in the stream in the absence of ultrasound, while Fig. 3(d) shows the bubbles in the presence of ultrasound.

Note that in the absence of ultrasound the bubbles exist as a large swarm or cloud. When ultrasound is applied they are attracted to each other to form clusters, which generate areas of high bubble activity (with associated microstreaming and shear) on the surface of the glass – one such area is arrowed in Fig. 3(d) (see also ESI†). The use of electrochemistry for the generation of the bubble swarm has many advantages. First, the apparatus needed within the cone is relatively non-invasive (here we employ two Pt microwire electrodes, 100  $\mu\text{m}$  in diameter stretching across the flow pattern developed at the nozzle mouth) compared to other technologies (for example direct injection through a needle or alternate acoustic sources).



**Fig. 3** Images to illustrate the pulsed electrochemical bubble swarm approach. (a) Schematic of the timing sequence. (b) Schematic of the processes involved showing the bubble swarm moving through the liquid to the substrate and then being activated. In this case the device is in a vertical orientation. (c) An image of a bubble swarm in the stream prior to activation. The dashed line highlights the edge of the stream as it impinges on a glass substrate and represents approximately 10 mm diameter. (d) Active bubble clusters on the substrate under the action of ultrasound. One such cluster is arrowed. Video showing three cycles of the process is available as ESI.† In this case the timing sequence was:  $t_{ec} = 10$  ms,  $t_{delay} = 25$  ms,  $t_{us} = 65$  ms (see (a) for definitions). The current passed to generate the bubble cloud was approximately 100 mA.

Second, the timing of the electrochemical generation can be controlled precisely with respect to the sound field and can be rapidly initiated and terminated as desired (within the limitations imposed by the electrochemical cell produced). Third, the amount of gas produced is directly related to the current passed and hence Faraday's law can be invoked to estimate the gas volume generated in any one pulse at the electrodes. While the advantages of the electrochemical generation are clear, one further consideration particularly pertinent to the cleaning arena should be considered; what is the size of the bubbles produced in this approach? For ultrasonic cleaning the coupling between the sound field and the bubbles is paramount. Ideally the best approach would be to choose a bubble size distribution so that

the resonant size of the bubbles present is as close as possible to the sound field employed. Under these conditions the acoustic coupling between the sound field and the bubbles will be optimal.<sup>30–33</sup> Hence, volumetric pulsations will be likely to lead to high oscillation amplitudes and consequently under certain conditions<sup>33–36</sup> to lead to surface waves<sup>32,33,37</sup> and in turn high local shear rates.<sup>13,29</sup> These are known to be useful in altering the local media (through lysis for example). In the work reported here the frequency used equates to a resonant radius of approximately 20  $\mu\text{m}$ . In order to investigate the size of bubbles generated electrochemically, separate experiments employing a thin layer flow cell and an electrochemical bubble generator similar to the geometry used in the cleaning device were performed. This enabled the visualisation of the bubble size distribution within the EBS. Fig. 4 shows the effect of the solution conditions (particularly surfactant loading) on the bubbles that can be produced. In this experiment electrolysis of water containing 0.1 M  $\text{Na}_2\text{SO}_4$  was investigated as a function of the surfactant (sodium dodecyl sulfate, SDS) loading of the system.<sup>38</sup> Fig. 4(a) shows that in the absence of SDS, relatively large bubbles are produced (of the order of 200  $\mu\text{m}$  in diameter). These are clearly much bigger than the desired size. However, the addition of SDS reduces the bubble size distribution significantly, as expected. It was found that 2 mM SDS produced bubbles with a size distribution suitable for the sound field employed. It is also interesting to consider the number of bubbles that would be produced under these conditions. If we assume an average bubble radius of 20  $\mu\text{m}$  in the presence of SDS, then a current of 100 mA (as used for the images shown in Fig. 3) will produce of the order of 50 000 bubbles per swarm in the 10 ms generation window.

Reducing the average size further increases this number but shifts the resonance size further from the optimal value for the sound field employed here. Further discussion and measurements of the exact bubble size distribution produced under these conditions is beyond the scope of this paper but will be discussed elsewhere.

Turning to the effect of these bubbles on surface cleaning, this paper will explore the device's performance where cleaning action due to the inherent acoustically activated bubble population generated by the flow system or the ultrasonic field is minimised. In order to do this we characterise the environment generated

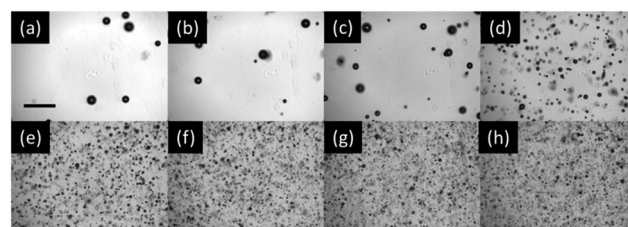


**Fig. 4** Images showing the effect of SDS surfactant loading on the bubble size distribution produced by two 100  $\mu\text{m}$  Pt electrodes in 0.1 M  $\text{Na}_2\text{SO}_4$ . In all cases the solution flowed over the electrodes at  $4 \text{ dm}^3 \text{ min}^{-1}$  with a 30 V potential generating  $\sim 280$  mA of current. The concentration of SDS in  $\mu\text{M}$  was 0, 1, 10, 100, 500, 1000, 2000, 5000 for images (a)–(h) respectively. The scale bar in frame (a) represents 800  $\mu\text{m}$ .

within the stream using an electrochemical sensor. Here we present the effect of the cleaning device on the re-passivation frequency recorded by an aluminium electrode under two sets of conditions. In the first, the acoustic pressure has been maximised while in the second, we reduce the pressure amplitude to a value of  $\sim 100$  kPa zero-to-peak. Under the lower pressure amplitude conditions, sensitive substrate materials are less likely to be affected by the device. Fig. 5 shows the effect of the acoustic pressure on the number of re-passivation events produced by the device employed here.<sup>39,40</sup> Fig. 5 shows that if the acoustic pressure is sufficiently high (see Fig. 5(a) for example), significant numbers of re-passivation events were detected by the aluminium electrode (up to 800 events per second using these conditions). However, if the acoustic pressure amplitude was reduced to  $\sim 100$  kPa (zero-to-peak) the frequency drops significantly to below  $1\text{ s}^{-1}$ . Fig. 5 also shows that the re-passivation of the aluminium surface is limited to a  $\sim 10$  mm diameter disk similar to the stream produced by the cleaning system. Clearly, even though re-passivation events

can be detected in both cases, controlling the pressure output has a marked effect on the frequency of re-passivation detected by the electrode within the stream. However, this does not indicate how effectively this system will behave for surface cleaning. In order to explore this issue, a set of cleaning experiments were performed. In this case, it was the intention to assess the effectiveness of the electrochemical bubble swarm at enhancing cleaning at a solid/liquid boundary using conditions of minimal re-passivation frequency (e.g.  $\sim 100$  kPa zero-to-peak amplitude). Fig. 6 shows a collection of results from these tests, which employed a fluorescent particle tracer as the contaminant. This contaminant is commercially available as an assay for hand-washing effectiveness. In the first test the sample was porcine skin. Fig. 6(a) shows a contaminated sample imaged under UV illumination. The contamination produces a green emission

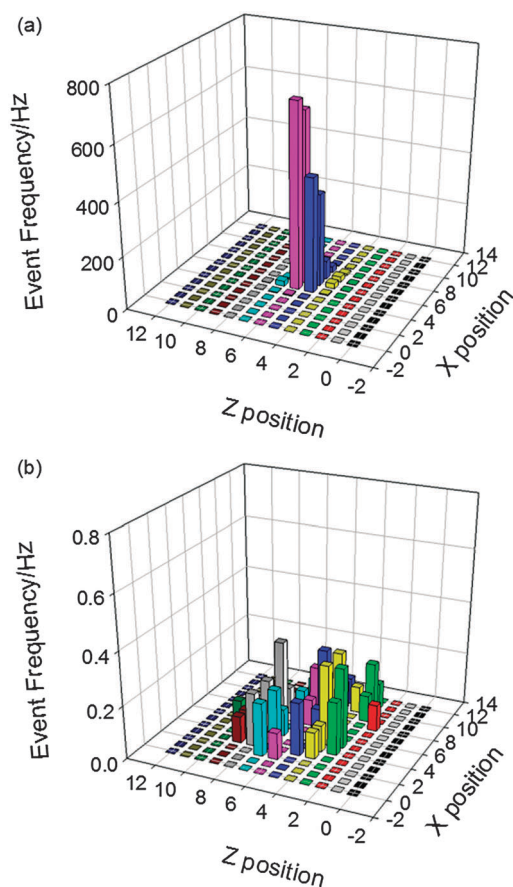


**Fig. 5** Plots showing the frequency of re-passivation events as a function of position in the stream for (a)  $\sim 245$  kPa (zero-to-peak) amplitude and (b)  $\sim 100$  kPa (zero-to-peak) amplitude. Note the different scales in each case. The solution contained 0.1 M  $\text{Na}_2\text{SO}_4$  and 2 mM sodium dodecyl sulphate. The sensing electrode was a 250  $\mu\text{m}$  diameter Al disc positioned 10 mm from the nozzle exit and then scanned in the XZ plane where 5,5 represents the centre of the stream. XZ scales in mm. In these cases no electrochemical bubbles were generated but the pulse regime was:  $t_{\text{ec}} = 10$  ms,  $t_{\text{delay}} = 25$  ms,  $t_{\text{us}} = 65$  ms.

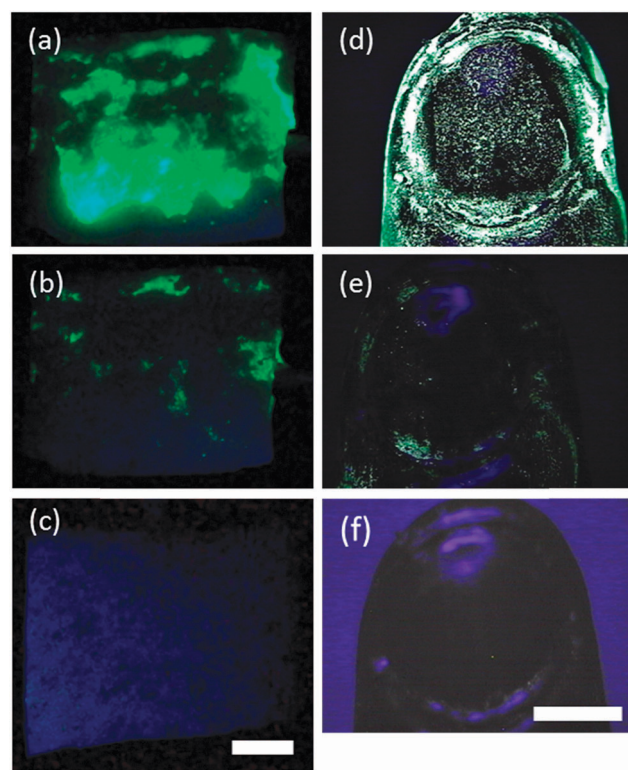


**Fig. 6** Images showing the effect of electrochemical bubble swarms on the removal of fluorescent particles. Image (a) shows a contaminated porcine skin sample. (b) Shows the same sample after exposure to the stream in the presence of ultrasound but without the addition of an electrochemical bubble swarm. (c) Shows another sample after exposure to the stream in the presence of ultrasound with the addition of an electrochemical bubble swarm. Image (d) shows a contaminated finger-mimic sample. (e) Shows the same sample after exposure to the stream in the presence of ultrasound but without the addition of an electrochemical bubble swarm. (f) Shows another sample after exposure to the stream in the presence of ultrasound with the addition of an electrochemical bubble swarm. Scale bars represent  $\sim 5$  mm. In all cases the solution contained 0.1 M  $\text{Na}_2\text{SO}_4$  and 2 mM sodium dodecyl sulphate, the acoustic pressure was  $\sim 100$  kPa zero-to-peak amplitude (measured  $\sim 10$  mm from the nozzle exit), the samples were held by hand approximately 10 mm from the nozzle exit and the exposure time was 10–15 s. The bubble pulse regime was  $t_{\text{ec}} = 10$  ms,  $t_{\text{delay}} = 25$  ms,  $t_{\text{us}} = 65$  ms. The current passed to generate the bubble cloud was approximately 100 mA.

under these conditions. Fig. 6(b) shows the same sample after exposure to the stream in the presence of ultrasound but without the addition of an electrochemical bubble swarm. There has been some removal of the contaminant but clearly much remains on the surface under the conditions employed. This limited removal indicates that there is a low level of inherent bubble cleaning activity in the stream under the conditions used. This can be compared with Fig. 6(c), which shows a separate sample after exposure to the stream in the presence of ultrasound with the addition of an electrochemical bubble swarm. Here it appears that, under the imaging used, the contaminant is totally removed from the surface. Note that in Fig. 6(c) the brightness of the image has been increased relative to Fig. 6(a) and (b) to allow the substrate and particles (if present) to be seen more clearly. This example clearly illustrates the significant enhancement in cleaning that the addition of an electrochemical bubble swarm can generate. Fig. 6(d–f) shows another example. In this case the substrate was a finger-mimic. Similar to the example above, the images show the contaminated sample (Fig. 6(d)), the sample after exposure to the activated stream in the absence of bubbles (Fig. 6(e)) and another sample after exposure to the activated stream in the presence of bubbles (Fig. 6(f)). Again, it is clear that the presence of the EBS leads to a significant improvement in the cleaning performance. This example is also interesting as it highlights the ability of the bubble swarms to clean in complex geometries such as those around the fingernail. In terms of mechanistic detail local shear and microstreaming, generated by the acoustically-induced bubble wall dynamics (see Fig. 3(d) and the ESI,† which shows the motion of the bubble swarm driven by the sound field employed), clean close to the bubble, and acoustic radiation forces drive the bubble onto the surface to be cleaned and into any cracks and crevices on it. Although it has been shown above that under the conditions used here bubble swarms are useful for surface cleaning there are some disadvantages of this approach. First, in order to generate the bubble swarm in the manner described here, an ionically conducting fluid is required. In the example shown an electrolyte was added, which may be detrimental or undesired under some circumstances. Second, the requirement of a surfactant to control the bubble sizes produced in the electrochemical generation of the bubble swarm could be problematic. However, the concentration of this species is minimal and has the added advantage in that this will aid the release of hydrophobic materials from the surface of the substrate to be cleaned. Third, in this pulsed mode operation, ultrasonic activation is only achieved 65% of the time which reduces the time that the surface is ensonified. Whilst this in principle could increase the cleaning times, it might be recalled that a simple pro rata calculation would not take into account the fact that pulsing a sound field can generate periods of activity greater than are observed in continuous-wave insonification, such that some pulsed regimes have been more active overall than continuous wave ones. Clearly the cleaning efficacy has improved under low acoustic amplitude conditions (as demonstrated by Fig. 6(c) and (f)) in the presence of the EBS). Finally, some discussion on the mechanistic details associated with the surface cleaning phenomena presented here is pertinent.

The effects of cavitation on a surface can be dramatic with microjets<sup>41–43</sup> and shockwaves<sup>14</sup> contributing to the effects at the interface. The contribution of bubble dynamics and the associated shear<sup>13,29</sup> may also impart significant cleaning action at the interface. These cleaning mechanisms will be driven by the application of an appropriate pressure field (such as that described here). However, the exact contribution of each mechanism in the UAS system requires further non-trivial experimental work. Nevertheless at a ~100 kPa zero-to-peak pressure amplitude (such as employed in the work reported in Fig. 6), the cleaning enhancement by the addition of the EBS is apparent while the effects on electrode depassivation minimal. This indicates that the contribution of this cloud (and the ensuing mechanisms associated with these generated bubbles) cannot be ignored.

## Conclusions

The addition of a controlled electrochemically generated bubble swarm to the output stream of an ultrasonic cleaning nozzle has been demonstrated with a small relatively non-invasive generator. This addition, which is able to respond rapidly and be coordinated with the excitation of bubble swarm produced using ultrasonic irradiation, has been shown to enhance surface cleaning of fluorescent particles loaded onto skin and finger-mimic interfaces. Bubble gating, as a result of the perturbation of the sound transmission through the cone and stream, is reported. However, this can be mitigated through the use of a pulsed approach. Finally control of the bubble swarm produced can be achieved through the appropriate use of solution conditions (here the presence of a suitable surfactant) to enable a suitable bubble size distribution to be realised.

## Acknowledgements

This work was supported by the Royal Society Brian Mercer Award for Innovation and Ultrawave Ltd for which the authors are extremely grateful. Data supporting this study are openly available from the University of Southampton repository at <http://dx.doi.org/10.5258/SOTON/379557>.

## Notes and references

- 1 S. E. Bilek and F. Turantaş, *Int. J. Food Microbiol.*, 2013, **166**, 155–162.
- 2 H. Murdoch, D. Taylor, J. Dickinson, J. T. Walker, D. Perrett, N. D. H. Raven and J. M. Sutton, *J. Hosp. Infect.*, 2006, **63**, 432–438.
- 3 I. J. Seymour, D. Burfoot, R. L. Smith, L. A. Cox and A. Lockwood, *Int. J. Food Sci. Technol.*, 2002, **37**, 547–557.
- 4 A. Kumar, R. B. Bhatt, P. G. Behere and M. Afzal, *Ultrasonics*, 2014, **54**, 1052–1056.
- 5 S. I. Nikitenko, L. Venault, R. Pflieger, T. Chave, I. Bisel and P. Moisy, *Ultrason. Sonochem.*, 2010, **17**, 1033–1040.
- 6 K. Perakaki, A. C. Mellor and A. J. E. Qualtrough, *J. Hosp. Infect.*, 2007, **67**, 355–359.

- 7 M. Hauptmann, S. Brems, H. Struyf, P. Mertens, M. Heyns, S. De Gendt and C. Glorieux, *Rev. Sci. Instrum.*, 2012, **83**, 034904.
- 8 M. Hauptmann, H. Struyf, P. Mertens, M. Heyns, S. De Gendt, C. Glorieux and S. Brems, *Ultrason. Sonochem.*, 2013, **20**, 77–88.
- 9 T. G. Leighton, *The Acoustic Bubble*, Academic Press, London, 1994.
- 10 P. R. Birkin, D. G. Offen, P. F. Joseph and T. G. Leighton, *J. Phys. Chem. B*, 2005, **109**, 16997–17005.
- 11 P. R. Birkin, R. O'Connor, C. Rapple and S. S. Martinez, *J. Chem. Soc., Faraday Trans.*, 1998, **94**, 3365–3371.
- 12 E. Maisonhaute, C. Prado, P. C. White and R. G. Compton, *Ultrason. Sonochem.*, 2002, **9**, 297–303.
- 13 J. A. Rooney, *Science*, 1970, **169**, 869–871.
- 14 A. Philipp and W. Lauterborn, *J. Fluid Mech.*, 1998, **361**, 75–116.
- 15 P. R. Birkin, D. G. Offen and T. G. Leighton, *Electrochem. Commun.*, 2004, **6**, 1174–1179.
- 16 D. G. Offen, *Acoustoelectrochemical characterisation of cavitation and its use in the study of surface processes*, PhD thesis, University of Southampton, 2006.
- 17 P. R. Birkin, D. G. Offen and T. G. Leighton, *Wear*, 2005, **258**, 623–628.
- 18 K. S. Suslick, *Sci. Am.*, 1989, **260**, 80–86.
- 19 E. B. Flint and K. S. Suslick, *Science*, 1991, **253**, 1397–1399.
- 20 K. S. Suslick, *Science*, 1990, **247**, 1439–1445.
- 21 T. J. Matula, R. A. Roy, P. D. Mourad, W. B. McNamara and K. S. Suslick, *Phys. Rev. Lett.*, 1995, **75**, 2602–2605.
- 22 G. J. Price and E. J. Lenz, *Ultrasonics*, 1993, **31**, 451–456.
- 23 P. R. Birkin, J. F. Power, A. M. L. Vinc and T. G. Leighton, *Phys. Chem. Chem. Phys.*, 2003, **5**, 4170–4174.
- 24 University of Southampton, Cleaning apparatus and method, and monitoring thereof, International Patent application PCT/EP, 2010/062448 filed 26 August 2010, Published 03 March 2011 under WO 2011/023746, Claiming priority from GB 0914836.2.
- 25 T. G. Leighton, P. R. Birkin and D. G. Offen, *Proc. Int. Congr. Acoust.*, 2013, **19**, 4.
- 26 J. B. Lonzaga, D. B. Thiessen and P. L. Marston, *J. Acoust. Soc. Am.*, 2008, **124**, 151–160.
- 27 J. B. Lonzaga, C. F. Osterhoudt, D. B. Thiessen and P. L. Marston, *J. Acoust. Soc. Am.*, 2007, **121**, 3323–3330.
- 28 P. R. Birkin, D. G. Offen, C. J. B. Vian, R. P. Howlin, J. I. Dawson, T. J. Secker, R. C. Hervé, P. Stoodley, R. O. C. Oreffo, C. W. Keevil and T. G. Leighton, *Phys. Chem. Chem. Phys.*, 2015, DOI: 10.1039/C5CP02406D.
- 29 A. R. Williams, D. E. Hughes and W. L. Nyborg, *Science*, 1970, **169**, 871–873.
- 30 T. G. Leighton, D. G. Ramble and A. D. Phelps, *J. Acoust. Soc. Am.*, 1997, **101**, 2626.
- 31 P. R. Birkin, Y. E. Watson and T. G. Leighton, *Chem. Commun.*, 2001, 2650–2651.
- 32 P. R. Birkin, Y. E. Watson, T. G. Leighton and K. L. Smith, *Langmuir*, 2002, **18**, 2135–2140.
- 33 Y. E. Watson, P. R. Birkin and T. G. Leighton, *Ultrason. Sonochem.*, 2003, **10**, 65–69.
- 34 A. O. Maksimov and T. G. Leighton, *Acustica*, 2001, **87**, 322–332.
- 35 R. Nabergoj and A. Francescutto, *J. Phys.*, 1979, **40**, C8-306–C8-309.
- 36 A. O. Maksimov and T. G. Leighton, *Proc. R. Soc. A*, 2012, **468**, 57–75.
- 37 D. G. Offen, P. R. Birkin and T. G. Leighton, *Electrochem. Commun.*, 2007, **9**, 1062–1068.
- 38 N. P. Brandon and G. H. Kelsall, *J. Appl. Electrochem.*, 1985, **15**, 475–484.
- 39 P. R. Birkin, D. G. Offen, C. J. B. Vian and T. G. Leighton, *J. Acoust. Soc. Am.*, 2011, **130**, 3379–3388.
- 40 C. J. B. Vian, P. R. Birkin and T. G. Leighton, *Anal. Chem.*, 2009, **81**, 5064–5069.
- 41 M. S. Plesset and R. B. Chapman, *J. Fluid Mech.*, 1971, **47**, 283.
- 42 O. Lindau and W. Lauterborn, *J. Fluid Mech.*, 2003, **479**, 327–348.
- 43 W. Lauterborn and H. Bolle, *J. Fluid Mech.*, 1975, **72**, 391.